IEEE Access
Multidisciplinary ⋮ Rapid Review ⋮ Open Access Journal

Received 22 June 2023, accepted 21 July 2023, date of publication 27 July 2023, date of current version 9 August 2023.

Digital Object Identifier 10.1109/ACCESS.2023.3299239

RESEARCH ARTICLE

Fading-Free 5G New Radio mm-Waves Generation Using Photonic Integrated Frequency Combs

EDUARDO SAIA LIMA[1,2], TOMÁS POWELL VILLENA ANDRADE[2], NICOLA ANDRIOLLI[3], EVANDRO CONFORTI[4], (Life Senior Member, IEEE), GIAMPIERO CONTESTABILE[5], AND ARISMAR CERQUEIRA S. JR.[2]

[1]VS Telecom, São Paulo 37540-000, Brazil
[2]Laboratory Wireless and Optical Convergent Access (WOCA), National Institute of Telecommunications (Inatel), Santa Rita do Sapucaí 37540-000, Brazil
[3]CNR-IEIIT, 56122 Pisa, Italy
[4]DECOM—University of Campinas, Campinas 13083-970, Brazil
[5]Scuola Superiore Sant'Anna, 56124 Pisa, Italy

Corresponding author: Nicola Andriolli (nicola.andriolli@cnr.it)

This work was supported in part by the Rede Nacional de Ensino e Pesquisa (RNP)-Ministério da Ciência, Tecnologia e Inovação (MCTIC), under the 6G Project, Conselho Nacional de Desenvolvimento Científico e Tecnológico (CNPq), Coordenação de Aperfeiçoamento de Pessoal de Nível Superior (CAPES), Financiadora de Estudos e Projetos (FINEP), and Fundação de Amparo à Pesquisa do Estado de Minas Gerais (FAPEMIG), under Grant 01245.010604/2020-14; in part by the Fundação de Amparo à Pesquisa do Estado de São Paulo (FAPESP) under Contract 21/06569-1 and Contract 15/24517-8; in part by CNPq under Grant 402471-2021-0; in part by the European Union under the Italian National Recovery and Resilience Plan (NRRP) of NextGenerationEU, Partnership on "Telecommunications of the Future" under Grant PE00000001-Program "RESTART."

ABSTRACT We experimentally demonstrate the use of an integrated optical frequency comb (OFC) for remotely generating low-phase noise millimeter-waves (mm-waves) carriers. The Indium Phosphide (InP) device is composed of phase modulators in tandem and is configurable in OFC center frequency and tone spacing. The device is applied in a centralized radio access network (C-RAN) architecture and the realized OFC is transported over 12.5 km of a conventional single-mode fiber (SMF) link aiming to remotely generate mm-waves. The impairments induced by the chromatic dispersion (CD) on the photodetected electrical carriers are evaluated, i.e., the periodic RF power fluctuations based on the electrical frequency and the SMF length. Experimental results demonstrate that, by properly managing the phase modulator bias and the phase delay supplied to the PIC, the impact of CD on the electrical carriers can be significantly reduced, leading the optical frequency comb to sum up in-phase after the photodetection process. The OFC-based and remotely generated carrier at 28 GHz is used to up-convert a 100 MHz 5G new radio (NR) signal, demonstrating suitable root mean square error vector magnitude (EVM_{RMS}) performance. Indeed, the OFC-based 5G NR signals met the 3GPP requirements with margins up to 7.7%, which enables the 5G wireless link at 28 GHz. Therefore, the proposed system is able to remotely generate mm-waves signal while minimizing the fading impact on the electrical signals, allowing to replace high-frequency up-converters at the remote 5G radio units.

INDEX TERMS 5G, fading-free mm-waves generation, low phase noise, optical frequency comb (OFC), photonic integrated circuits (PIC).

I. INTRODUCTION

In the last years, the continuously improving wireless technology standards had huge positive impacts on society and industry, which are expected to increase in the upcoming years with the fifth and the sixth generations of mobile networks (namely 5G and 6G). 5G enables new value-added applications, encompassing enhanced mobile broadband (eMBB), ultra-reliable and low-latency communications (URLLC), and also massive machine-type communications (mMTC) [1]. The 5G radio access network (RAN) has been commercially deployed around the globe, initially in a non-standalone (NSA) mode using the control plane of the legacy networks, and then in a standalone (SA)

The associate editor coordinating the review of this manuscript and approving it for publication was David Caplan.

implementation, enabling the full 5G capabilities [2]. In parallel to the 5G deployment, the sixth generation of mobile services (6G) already started to be developed worldwide, planning to provide further enhanced performance and efficiency to the future demands [3].

5G as well as 6G trends concern the use of high operating frequencies, and consequently, bandwidths. In this regard, several frequency ranges have been standardized for the 5G New Radio (5G NR) interface, including frequency range 1 (FR1) from 410 MHz to 7.125 GHz and frequency range 2 (FR2) from 24.25 GH to 52.6 GHz [2]. The huge amount of spectrum available in FR2 enables 5G mm-wave access points using up to 400 MHz bandwidths, aiming to achieve Gbit/s throughput [4]. Along the same lines, 6G prospects indicate higher bandwidths and frequencies to reach communications beyond Gbit/s. As a consequence, advanced techniques for generating mm-waves and THz signals with high spectral purity and low phase noise are mandatory [5]. However, purely electronic-based oscillators are typically bulky, power-hungry, and expensive. In this context, photonics-based frequency generation is attractive to enable optical-wireless convergence by optically generating and distributing mm-waves and THz signals [6], [7].

Among the photonics-based techniques for mm-waves generation, heterodyne detection is the most used scheme, requiring phase coherence between two optical tones to generate low-phase-noise electrical signals at a frequency equal to the spacing between the two optical carriers [8]. Although the heterodyne mechanism is relatively straightforward, the use of uncorrelated optical carriers generates noisy RF signals. For this reason, additional techniques and devices are required to obtain coherently locked tones and, consequently, low-phase-noise mm-wave signals.

Photonic-assisted generation of mm-wave signals has been reported using a dual-wavelength mode-locked laser (MLL) [9], optical injection locking (OIL) [10], and optical phase-lock loop (OPLL) [11] to establish the carrier phase correlation. Optical frequency multiplication (OFM) techniques based on external modulation (EM) have also been reported [12], [13]. An alternative approach for generating mm waves exploits optical frequency combs (OFC). An OFC consists of a series of optical spectral tones, equally spaced and coherent in phase, generated by a single device or subsystem [14]. Comb-based mm-wave generation is the most flexible technique since, if necessary, it can provide multiple frequencies with the very same device, and it requires a much lower electrical input frequency compared to other approaches as it inherently performs an N-time frequency multiplication. Different sources and effects have been used to generate OFCs, including mode-locked lasers [15], Kerr-based approaches exploiting multiple four-wave mixing (FWM) or micro-resonators [16], [17], and also electro-optic modulators [18], [19].

Each solution has pros and cons in consideration of the particular application. Although electro-optic frequency combs are typically characterized by a smaller frequency spacing in respect of the previously presented techniques, this scheme offers suitable noise properties, since it is based on the noises from the laser and RF sources. In addition, such a technique provides remarkable flexibility in terms of comb wavelength and frequency spacing, and a huge potential for photonic integration [20], [21], all of which are key features for the 5G and 6G network deployment. In addition, recent progress on integrated photonics [22], a research field focused on miniaturizing and integrating multiple optical components on a chip [23], has indicated the huge potential of photonic integrated circuits (PIC). Table 1 reports the state-of-the-art on photonics-based frequency generation and multiplication.

TABLE 1. Electrical signal generation based on photonic techniques.

Ref	Frequency	Method	PIC	Link distance	Application
[24]	6 GHz	External modulation	no	1.5 km	Mobile
[25]	100 GHz	External modulation	no	-	-
[10]	101.7 GHz	Optical injection locking	yes	-	-
[11]	45.4 GHz	Optical phase-lock loop	no	-	-
[26]	93 GHz	Optical injection locking	yes	-	-
[27]	36 GHz	Kerr comb	-	no	-
[28]	10/20 GHz	Microcomb	yes	-	Radar
[29]	47 GHz	Dual-wavelength distributed feedback laser	yes	25-50km	5G FR2
This work	**28 GHz**	**Electro-optic OFC**	**yes**	**12.5 km**	**5G FR2**

Comparing this work with the literature, just a few works used PICs or integrated OFC for generating mm-waves, the most part employed bench-top components. In addition, a small fraction of them focuses on the remote generation, considering the optical fronthaul link, therefore, removing the impairments induced by chromatic dispersion (CD). Lastly, most of the works focused only on the comb generation, without demonstrating the application of the generated mm-wave signals. In addition, our previous work [30] focused only on the low-phase-noise mm-wave generation using the integrated OFC, without the transmission across an optical fiber link as well as the 5G up-conversion and evaluation. With respect to [31], we have enhanced the OFC generation by including an electrical amplifier at the phase modulator (PM) input, and we have studied and minimized the impact of chromatic dispersion on the photonics-based remotely-generated mm-wave signals. Accordingly, this work stands out as a full-fledged 5G deployment, encompassing the remote low-phase-noise mm-wave generation based on integrated OFC, the use of a 12.5 km optical fiber link, the up-conversion and performance evaluation of a 28 GHz 5G new radio (NR) signal, demonstrating the feasibility of the proposed system to enable 5G mm-wave hotspots.

II. PHOTONIC INTEGRATED FREQUENCY COMB

Multiple photonic integration technologies have been developed in the last years: the Indium Phosphide (InP) platform is particularly suited for telecom and microwave photonics applications since it allows the monolithic integration of many active and passive components, ranging from lasers, modulators, waveguides, detectors, etc.

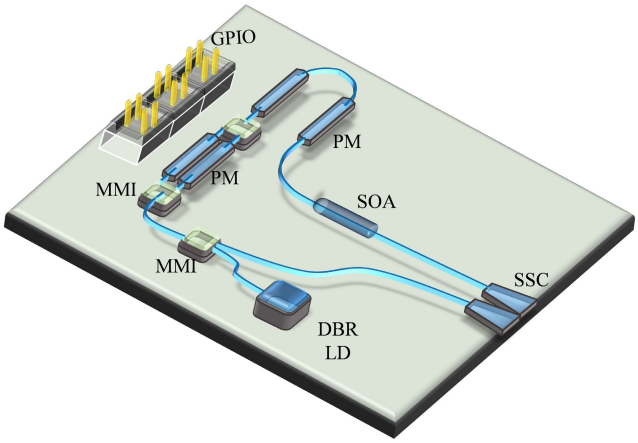

FIGURE 1. Integrated optical frequency comb schematic. Distributed Bragg reflector laser diode (DBR-LD); multi-mode interference (MMI); phase modulator (PM); general purpose Input/Output (GPIO); semiconductor optical amplifier (SOA); spot-size converter (SSC).

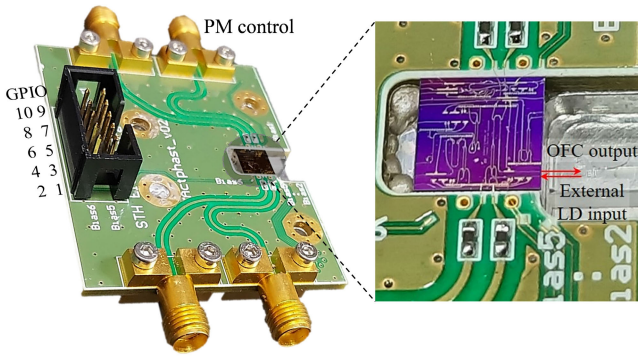

FIGURE 2. PIC mounted on a metal chuck and assembled with a custom-designed printed circuit board; zoom-in-view of the chip.

Fig. 1 presents the block diagram of the InP photonic integrated frequency comb. The device was designed and fabricated in a multi-project wafer run, using a generic integration technology [32]. It was initially characterized in [20] and [21]: in this work it is applied to remotely generate mm-waves and up-convert a 5G signal. A continuous-wave (CW) light source is used to provide a seed signal for OFC generation, setting also the OFC central frequency. For this purpose either an on-chip distributed Bragg reflector laser diode (DBR-LD) or an external laser diode can be exploited. Spot-size converters (SSCs) positioned at the PIC edge allow the coupling of the external laser and of the OFC output while minimizing insertion losses.

The coupling and splitting of the light in the PIC are performed by multi-mode interference (MMI) devices. After the DBR-LD and the input SSC, a 2 × 1 MMI is used to combine the CW light sources. Afterward, the optical carrier is sent to a dual-drive Mach-Zehnder modulator (DD-MZM), which modulates the optical signal in amplitude. The MZM consists of a 1 × 2 MMI splitter, followed by two phase modulators (PM), and an identical MMI used as a combiner. The PMs exploit the quantum confined Stark effect, resulting in a bandwidth of 7-GHz and a V_π of 5 V. After crossing the DD-MZM, two further cascaded PMs are used to induce a phase modulation, increasing the modulation index and thus the OFC bandwidth. Finally, a 500-μm long semiconductor optical amplifier (SOA) based on a multi-quantum-well structure is used to amplify the generated OFC. The SOA emission is centered at 1535 nm with a bandwidth of 62 nm.

Fig. 2 shows the photograph of the assembled photonic integrated circuit and a zoom-in view of the chip. The PIC is mounted on a metal chuck and connected via wire bonds to a custom-designed printed circuit board (PCB). Four RF ports are connected to the PM sections, whereas a GPIO is used to feed the DBR-LD sections and the SOA. The chip size is approximately 5 × 5 mm^2, however, the effective footprint of the PIC is approximately 4.5 × 2.5 mm^2. The integrated chip also comprises additional test DBR-LDs, SOAs, and PMs used to qualify the fabrication process and simplify the characterization of the individual components.

III. INTEGRATED OFC APPLIED TO FADING-FREE REMOTE 5G MM-WAVE GENERATION

Fig. 3 describes the experimental setup employed to demonstrate the fading-free remote mm-wave generation assisted by an integrated OFC. The device has been positioned in a centralized radio access network (C-RAN) scheme, more specifically, in a central office (CO), aiming to generate and transport the OFC. At the remote station (remote radio unit, RRU), the OFC optically generates low-phase-noise mm-waves, aiming to replace expensive, power-hungry, and bulky high-frequency oscillators. To generate a wide and clean optical frequency comb, phase modulators must be driven with in-phase RF signals and the proper DC bias voltages. The RF signal frequency dictates the OFC spacing, whereas the RF and bias voltages directly impact the number and the flatness of the comb lines.

Initially, a 4-GHz sinusoidal signal has been provided by an RF generator (Keysight E8267D) at the central office, which dictates the optical frequency comb spacing. The signal has been amplified and divided into four by means of an electrical amplifier (EA) and a splitter, respectively. The phases have been adjusted by using phase shifters (PS). Four bias tees combined the 4-GHz electrical signals with the DC signals. The cascaded PMs have been driven with multiples of V_π to maximize the modulation index and thus the comb bandwidth, whereas the dual-drive Mach- Zehnder modulator with V_π to optimize the comb shape [18].

Concerning the PIC output, a high numerical aperture fiber array has been accurately aligned at the chip edge employing a 3-axis micro-positioner, since the OFC emission occurs via free-space optics (FSO). The fiber array placement can be observed on the right-hand side of Fig. 2 with the red arrows highlighting the OFC output port and the external laser input port. The comb output power was around -2 dBm, measured using a wide-area detector, whereas the fiber-coupled optical

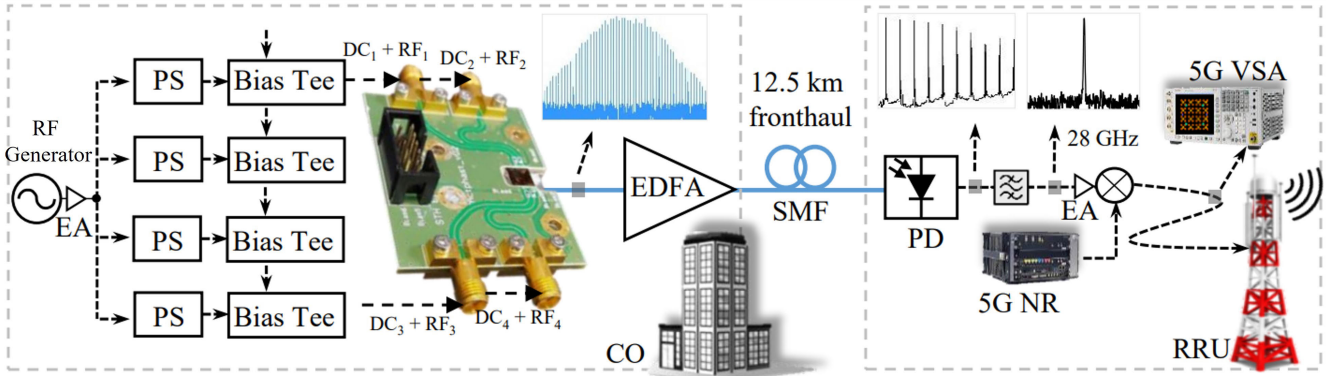

FIGURE 3. Block diagram of the proposed photonics-based remote 5G mm-waves generations based on an integrated OFC. Electrical amplifier - EA; PS - phase shifter; Erbium-doped fiber amplifier - EDFA; central office (CO) single-mode fiber - SMF; PD - photodetector; vector signal analyzer - VSA; remote radio unit - RRU.

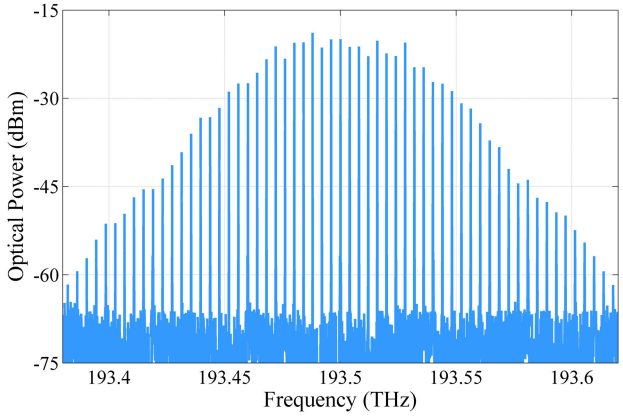

FIGURE 4. 4-GHz spacing OFC obtained by the heterodyne detection technique.

power was around -7 dBm, resulting in 5 dB losses caused by the coupling/alignment. After the proper alignment, an optical spectrum analyzer (OSA) (Anritsu MS9740A) has been used to measure the optical frequency comb. However, the OSA resolution is 0.07 nm, enabling the visualization of optical frequencies spaced by at least 9 GHz. Aiming to overcome the coarse OSA resolution, we have used a heterodyne detection technique followed by MATLAB processing to accurately image the OFC. For this purpose, we have considered the CSV files of the optical spectrum envelope measured by the OSA, the electrical frequency comb measured by the high-speed PD, and the main PD features.

Fig. 4 presents the resulting optical frequency comb with 4 GHz frequency spacing. A relatively flat-top OFC can be appreciated, occupying around 240 GHz (193.38 THz up to 193.62 THz). Considering that the optical frequency comb noise floor is around -67 dBm, 21 frequencies reported an optical signal-to-noise ratio (OSNR) higher than 40 dB. We could achieve a flatter top comb by adding electrical amplifiers at the phase modulator input, however, a flat top comb is not required for the optical frequency multiplication application. Therefore, the variation observed in the flat part of the comb is higher than 1 dB. In any case, one can note 19 tones within 5 dB from the maximum and around 10 tones within a 3 dB range. Therefore, the OFC bandwidth and the strong phase correlation among the optical carriers are suitable for generating mm-wave signals.

After the proper OFC measurement, an Erbium-doped fiber amplifier (EDFA) was set with 12 dB gain to compensate for the losses caused by alignment and propagation, transmitting 5 dBm and reaching an optical power of around 2 dBm at the RRU side. The optical frequency comb was transmitted across a 12.5-km-long optical fronthaul of single-mode fiber, aiming to provide a remote photonics-based mm-wave generation by using a high-speed photodetector. However, it is well known that analog radio over fiber (A-RoF) transmissions may suffer from impairments induced by chromatic dispersion, which causes a periodic fluctuation of the RF output power known as signal fading [33]. For instance, considering a signal with frequency f_{RF} transmitted in an A-RoF link, the first power fading, i.e., a power null, occurs ideally at a first distance [33]:

$$L1 = \frac{c}{2D\lambda_0^2 f_{RF}^2}, \tag{1}$$

where D is the fiber linear dispersion parameter, λ_0 is the optical signal wavelength, and c is the speed of light. Sequentially, the null points will occur at each distance interval:

$$\Delta L = \frac{c}{D\lambda_0^2 f_{RF}^2}. \tag{2}$$

Fig. 5 presents a numerical evaluation regarding the fundamental electrical power fluctuation at the photodetector output in an A-RoF link as a function of the RF frequency. Two spans of standard SMF with $D = 17$ ps/nm·km have been considered: the experimental link length of 12.5 km and the maximum fronthaul link length of 20 km. Regarding the 12.5-km link, following the equations, one could expect fading points positioned at approximately 17.7, 30.6, 39.5 GHz, and so on. In addition, as expected, the link length

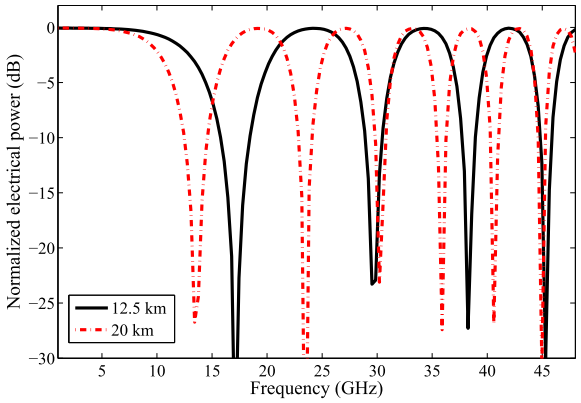

FIGURE 5. Photodetected electrical power as a function of the frequency for an analog RoF transmission for SMF links of 12.5 and 20 km.

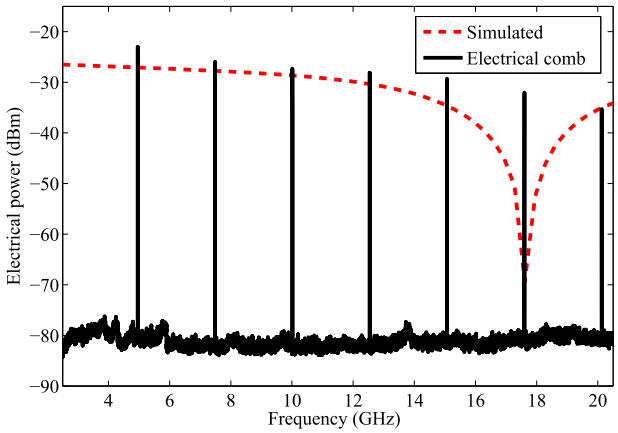

FIGURE 6. Generated electrical comb after 12.5-km of SMF and the fading nodes simulation for a 12.5-km A-RoF link.

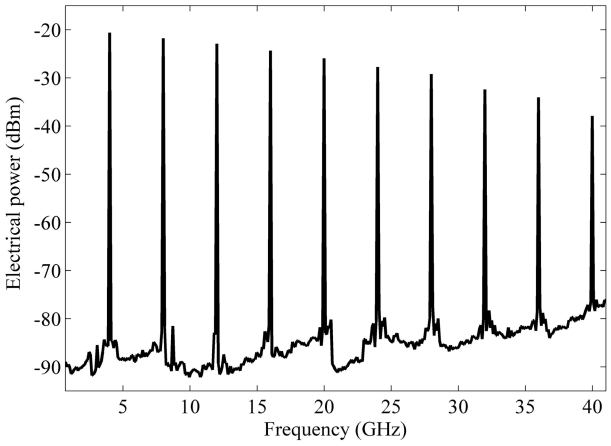

FIGURE 7. Electrical frequency comb spaced by 4 GHz.

increment directly impacts the periodicity of the nulls, which can be critical for long A-RoF links and the transport of high-frequency RF signals. Therefore, the photonics-based techniques to generate mm-waves or even THz must consider the impact of chromatic dispersion.

To evaluate the CD impact on the electrical comb generation, an optical frequency comb spacing of 2.5285 GHz has been selected, whose seventh harmonic, at 17.7 GHz, falls within a null after 12.5 km SMF propagation. Fig. 6 presents the generated electrical tones at the PD output, after 12.5 km of SMF link and the fading node simulation for the same distance. It is worth mentioning that in the first measurement, i.e., without parameters optimization, the electrical comb was not flat. However, adjustments to the phase modulator bias voltages and particularly to the phase shifters compensate for the phase deviations caused by the optical fiber link and drastically reduce the dispersion impact on the electrical carriers. Consequently, the resulting electrical carrier does not suffer from the fading effect when the PSs are properly adjusted, thus, the in-phase electrical carriers sum after the detection. Therefore, the proposed system is able to remotely generate mm-wave signals minimizing the fading impact on the electrical signals.

After the fading evaluation, we have set the optical frequency comb spacing to 4 GHz in order to remotely generate mm-wave carriers within the standardized 5G FR2 (24.25-52.6 GHz), more specifically at 28 GHz. Fig. 7 reports the electrical frequency comb measured at the photodetector output by a 43 GHz electrical spectrum analyzer (ESA). The average optical power was set to 2 dBm at the photodetector input. The PD is a 70 GHz Balanced Photodetector (BPDV3120R) with a maximum average optical input power of 16 dBm and a minimum responsivity of 0.45 A/W in the optimum polarization condition. A flat 4 GHz spaced electrical frequency comb can be appreciated with considerable electrical power and signal-to-noise ratio (SNR) ranging up to the mm-waves range. In addition, a slight RF power reduction as a function of the frequency can be observed, mainly due to the response of the components as well as the 1.5-m RF cable attenuation over the entire frequency range. Despite the power reduction, one could expect the electrical frequency comb can be used for the entire 5G FR2. It is worth mentioning that the phase modulators operate up to 7 GHz. Therefore, the approach can be employed in a wide range of applications, demanding only the management of the RF generator carrier frequency and the choice of the desired multiplication factor. In particular, our target was the 7-times multiplied electrical signal (28 GHz), which presented suitable power and SNR of around -28 dBm and 57 dB, respectively.

An ideal oscillator would produce a perfect sine wave, however, in practical applications the generated signal presents fluctuations in amplitude and phase. In particular, the phase fluctuations or the deviations from the ideal periodicity cause the phase noise (commonly expressed in dBc/Hz), which represents the noise power relative to the carrier in a certain frequency offset or simply the spectral density of the signal phase noise. In addition, the impact of the phase noise on the system performance increases for high frequency, since severe phase noise is caused and increased

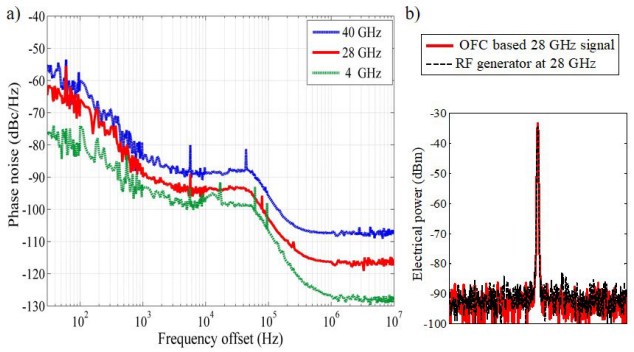

FIGURE 8. a) Phase noise measurements of the RF oscillator used as a source at 4 GHz and the remote optically-generated carriers operating at 28 GHz and 40 GHz. b) Comparison of the OFC-based carrier with a bench-top RF generator at 28 GHz with 500 kHz span.

by the loop synthesizers and active components operating at mm-waves. One of the main issues caused by phase noise into an orthogonal frequency-division multiplexing (OFDM) signal is a phase rotation of all the sub-carriers, denoted as common phase error (CPE) [34]. Consequently, phase tracking reference signals (PTRS) have been added in 5G NR systems for tracking the phase [2]. Although the PTRS reduces the impact of the phase noise on the system performance, mm-wave signals with low phase noise are still mandatory.

Then, we performed phase-noise measurements to evaluate the quality and stability of the photonics-based carriers generated at the remote radio unit. In our specific architecture, we have never experienced any instabilities due to thermal crosstalk effects on the PIC components and the comb generator response was not affected by small changes in the modulation index (dependent on the modulator V_π). In this way, no thermoelectric cooler (TEC) was required in the experiments since the device was fixed on a metal surface used as a heat sink, demanding just the control of the environmental temperature. Fig. 8 a) reports the phase noise measurements of the RF oscillator used as a source at 4 GHz and the photonics-based carriers operating at 28 GHz and 40 GHz. Considering the RF generator, a phase noise of around -76 dBc/Hz has been demonstrated for 1 kHz offset, whereas 28 GHz and 40 GHz reported -56 dBc/Hz and -63 dBc/Hz, respectively. In particular, the phase noise of optically multiplied signals using optical modulators is approximately the phase noise of the source added with $20log_{10}(m)$, being m the multiplication factor [25]. Therefore, the phase noise of the 28 GHz and the 40 GHz carriers approximately follow the phase noise of the oscillator at 4 GHz added $20log_{10}(7)$ and $20log_{10}(10)$, respectively, the expected phase noise increment at 28 GHz and 40 GHz can be appreciated. The last characterization consisted in comparing the spectra of the OFC-based carrier with a 28 GHz signal generated by the commercial Keysight E8267D RF generator, as reported in Fig. 8 b). We have set a practically equivalent electrical power and the measurement frequency span of around 500 kHz. The performance of the remote and optically generated carrier is similar to a bench-top 43-GHz electrical generator. Therefore, the integrated OFC provides coherent optical tones and consequently is able to provide configurable frequency multiplication with low phase noise.

For the subsequent system demonstration, the generated low-phase noise signal at 28 GHz was employed to up-convert a 5G NR signal and its performance was assessed. The 5G NR baseband signal is generated at the RRU, by the equipment denoted as 5G NR in Fig. 3. Fig. 9 shows a photograph of the complete experimental setup, which is in accordance with the description of Fig. 3. The 28 GHz signal was filtered and individually amplified. Afterward, the 5G NR signal provided by an arbitrary waveform generator (AWG) Keysight M9505A was up-converted to 28 GHz by using a mixer. The 5G signal configuration followed the 3rd Generation Partnership Project (3GPP) reports focused on user equipment. We have used bandwidths up to 100 MHz since it is the maximum demodulation bandwidth of the employed vector signal analyzer (VSA) M9020A MXA.

FIGURE 9. Photograph of the experimental setup.

The 5G downlink shared channels (DL-SCH) were modulated using 16-QAM and 64-QAM. The primary (PSS) and secondary synchronization signals (SSS) have also been configured, enabling the UE to receive the frame time and cell-id. The 28-GHz 5G NR was then evaluated by the VSA in terms of root mean square error vector magnitude (EVM_{RMS}). The 3GPP has defined maximum EVM values depending on the modulation, i.e., 8.0%, 12.5%, and 17.5% for 64-QAM, 16-QAM, and QPSK (quadrature phase-shift keying) schemes, respectively. Fig. 10 presents the EVM_{RMS} performance of the photonics-based 5G NR signal at 28 GHz as a function of the modulation index and signal bandwidth.

Considering 20-MHz bandwidth with 16-QAM, we have achieved 80 Mbit/s and EVM_{RMS} around 3.05%, whereas the

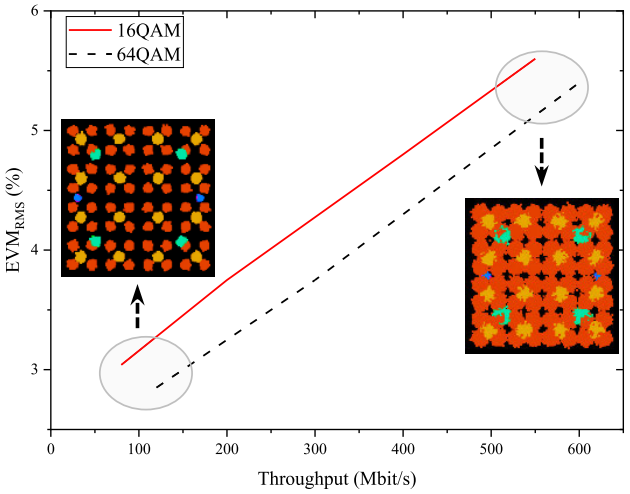

FIGURE 10. **EVM$_{RMS}$ evaluation of the photonics-based 5G NR signal at 28 GHz as a function of the modulation scheme and bandwidth.**

64-QAM provided 120 Mbit/s and EVM$_{RMS}$ around 2.85%. The received symbols in the constellation can be clearly distinguished. The synchronism symbols are represented in blue and green (BPSK) and QPSK modulation, whereas the data symbols are reported in orange tones with 16-QAM and 64-QAM. We have then increased the signal bandwidth and measured the obtained EVM$_{RMS}$ for multiple points. In the experiment, the optical and electrical power were kept the same, resulting in an electrical signal of around -18 dBm. Since we have only reconfigured the 5G bandwidth, i.e., from 10 MHz up to 100 MHz, and the channel power was always kept around -18 dBm, the bandwidth increment results in a slight SNR reduction, and consequently in an EVM degradation. For 100 MHz bandwidth the 64-QAM signal attained 600 Mbit/s with EVM$_{RMS}$ around 5.4 %, fulfilling the requirements with more than 2.6% of margin. In addition, the 16-QAM operating with 100 MHz bandwidth provided 400 Mbit/s and plenty of margins, i.e., 7.7%. To increase the throughput of the 16-QAM, we have occupied the bandwidth with 16- and 64-QAM signals, attaining around 550 Mbit/s. In general, the OFC-based 5G NR signals met the 3GPP requirements with margins up to 7.7%, which might be used to implement the 5G access points at 28 GHz. Therefore, the proposed approach for remote mm-wave generation has shown potential for integrating the 5G networks, aiming to replace high-frequency generators at the remote radio unit.

IV. CONCLUSION

We have successfully proposed and experimentally demonstrated the use of an integrated optical frequency comb generator for remotely generating mm-waves 5G signals. The Indium Phosphide OFC generator is composed of cascaded phase modulators and is adjustable in respect of OFC center and tone spacing. The photonic integrated circuit was applied in a C-RAN architecture and the generated OFC was transported in a 12.5 km SMF link aiming to remotely generate 5G signals at 28 GHz.

We have evaluated the impairments induced by the chromatic dispersion on the generated electrical carriers, which leads the RF output power to a periodic fluctuation known as signal fading. Despite the CD impact, the obtained results demonstrated that controlling the PM bias and the PSs intensely reduces the CD impact on the carriers, resulting in a relatively flat electrical comb without null points.

The OFC-based and remotely generated carrier at 28 GHz was then employed to up-convert a 100 MHz 5G new radio signal, which was evaluated in terms of EVM$_{RMS}$. The OFC-based 5G NR signals achieved 600 Mbit/s with EVM$_{RMS}$ margins up to 7.7%, which might be used to deploy an5G access point operating at 28 GHz, demonstrating the system feasibility to remotely generate mm-waves without CD impact, aiming to replace complex and high-frequency generator at the RRU. Future works regard the use of the PIC to generate a coherent dual-wavelength optical frequency comb, enabling the generation of higher frequencies up to sub-THz carriers.

REFERENCES

[1] S. Henry, A. Alsohaily, and E. S. Sousa, "5G is real: Evaluating the compliance of the 3GPP 5G new radio system with the ITU IMT-2020 requirements," *IEEE Access*, vol. 8, pp. 42828–42840, 2020.

[2] *Group Radio Access Network; NR; User Equipment (UE) radio transmission and reception; Part 1: Range 1 Standalone*, document TS 38.101-1, 3GPP, version 15.5.0, Release 15, 2019.

[3] S. Dang, O. Amin, B. Shihada, and M.-S. Alouini, "What should 6G be?" *Nature Electron.*, vol. 3, no. 1, pp. 20–29, Jan. 2020.

[4] T. S. Rappaport, S. Sun, R. Mayzus, H. Zhao, Y. Azar, K. Wang, G. N. Wong, J. K. Schulz, M. Samimi, and F. Gutierrez, "Millimeter wave mobile communications for 5G cellular: It will work!" *IEEE Access*, vol. 1, pp. 335–349, 2013.

[5] E. A. Kittlaus, D. Eliyahu, S. Ganji, S. Williams, A. B. Matsko, K. B. Cooper, and S. Forouhar, "A low-noise photonic heterodyne synthesizer and its application to millimeter-wave radar," *Nature Commun.*, vol. 12, no. 1, pp. 1–10, Jul. 2021.

[6] J. Capmany and D. Novak, "Microwave photonics combines two worlds," *Nature Photon.*, vol. 1, no. 6, pp. 319–330, Jun. 2007.

[7] I. Degli-Eredi, P. An, J. Drasbæk, H. Mohammadhosseini, L. Nielsen, P. Tønning, S. Rommel, I. T. Monroy, and M. J. R. Heck, "Millimeter-wave generation using hybrid silicon photonics," *J. Opt.*, vol. 23, no. 4, Apr. 2021, Art. no. 043001.

[8] J. Yao, "Microwave photonics," *J. Lightw. Technol.*, vol. 27, no. 3, pp. 314–335, Feb. 1, 2009.

[9] R. Li, H. Shi, H. Tian, Y. Li, B. Liu, Y. Song, and M. Hu, "All-polarization-maintaining dual-wavelength mode-locked fiber laser based on Sagnac loop filter," *Opt. Exp.*, vol. 26, no. 22, p. 28302, 2018.

[10] K. Balakier, M. J. Fice, F. van Dijk, G. Kervella, G. Carpintero, A. J. Seeds, and C. C. Renaud, "Optical injection locking of monolithically integrated photonic source for generation of high purity signals above 100 GHz," *Opt. Exp.*, vol. 22, no. 24, p. 29404, 2014.

[11] J.-P. Zhuang and S.-C. Chan, "Tunable photonic microwave generation using optically injected semiconductor laser dynamics with optical feedback stabilization," *Opt. Lett.*, vol. 38, no. 3, pp. 344–346, 2013.

[12] C.-T. Lin, P.-T. Shih, J. Chen, W.-J. Jiang, S.-P. Dai, P.-C. Peng, Y.-L. Ho, and S. Chi, "Optical millimeter-wave up-conversion employing frequency quadrupling without optical filtering," *IEEE Trans. Microw. Theory Techn.*, vol. 57, no. 8, pp. 2084–2092, Aug. 2009.

[13] W. Li and J. Yao, "Microwave and terahertz generation based on photonically assisted microwave frequency twelvetupling with large tunability," *IEEE Photon. J.*, vol. 2, no. 6, pp. 954–959, Dec. 2010.
[14] T. Fortier and E. Baumann, "20 years of developments in optical frequency comb technology and applications," *Commun. Phys.*, vol. 2, no. 1, pp. 1–16, Dec. 2019.
[15] H. A. Haus, "Mode-locking of lasers," *IEEE J. Sel. Top. Quantum Electron.*, vol. 6, pp. 1173–1185, 2000.
[16] A. C. S. Jr., J. M. C. Boggio, A. A. Rieznik, H. E. Hernandez-Figueroa, H. L. Fragnito, and J. C. Knight, "Highly efficient generation of broadband cascaded four-wave mixing products," *Opt. Exp.*, vol. 16, no. 4, pp. 2816–2828, 2008.
[17] J. Pfeifle, V. Brasch, M. Lauermann, Y. Yu, D. Wegner, T. Herr, K. Hartinger, P. Schindler, J. Li, D. Hillerkuss, R. Schmogrow, C. Weimann, R. Holzwarth, W. Freude, J. Leuthold, T. J. Kippenberg, and C. Koos, "Coherent terabit communications with microresonator Kerr frequency combs," *Nature Photon.*, vol. 8, no. 5, pp. 375–380, May 2014.
[18] A. J. Metcalf, V. Torres-Company, D. E. Leaird, and A. M. Weiner, "High-power broadly tunable electrooptic frequency comb generator," *IEEE J. Sel. Topics Quantum Electron.*, vol. 19, no. 6, pp. 231–236, Nov. 2013.
[19] M. Imran, P. M. Anandarajah, A. Kaszubowska-Anandarajah, N. Sambo, and L. Potí, "A survey of optical carrier generation techniques for terabit capacity elastic optical networks," *IEEE Commun. Surveys Tuts.*, vol. 20, no. 1, pp. 211–263, 1st Quart., 2018.
[20] N. Andriolli, T. Cassese, M. Chiesa, C. de Dios, and G. Contestabile, "Photonic integrated fully tunable comb generator cascading optical modulators," *J. Lightw. Technol.*, vol. 36, no. 23, pp. 5685–5689, Dec. 1, 2018.
[21] F. Bontempi, N. Andriolli, F. Scotti, M. Chiesa, and G. Contestabile, "Comb line multiplication in an InP integrated photonic circuit based on cascaded modulators," *IEEE J. Sel. Topics Quantum Electron.*, vol. 25, no. 6, pp. 1–7, Nov. 2019.
[22] D. Marpaung, J. Yao, and J. Capmany, "Integrated microwave photonics," *Nature Photon.*, vol. 13, no. 2, pp. 80–90, Feb. 2019.
[23] A. L. Gaeta, M. Lipson, and T. J. Kippenberg, "Photonic-chip-based frequency combs," *Nature Photon.*, vol. 13, no. 3, pp. 158–169, Mar. 2019.
[24] R. M. Borges, D. Mazzer, T. R. Rufino Marins, and A. C. Sodré, "Photonics-based tunable and broadband radio frequency converter," *Opt. Eng.*, vol. 55, no. 3, Dec. 2015, Art. no. 031118.
[25] W. Li and J. Yao, "Investigation of photonically assisted microwave frequency multiplication based on external modulation," *IEEE Trans. Microw. Theory Techn.*, vol. 58, no. 11, pp. 3259–3268, Nov. 2010.
[26] L. Gonzalez-Guerrero, R. Guzman, M. Ali, J. C. Cuello, D. Dass, C. Browning, L. Barry, I. Visscher, R. Grootjans, C. G. H. Roeloffzen, and G. Carpintero, "InP-Si_3N_4 hybrid integrated optical source for high-purity mm-wave communications," in *Proc. Opt. Fiber Commun. Conf.*, 2022, pp. 1–3.
[27] K. Saleh and Y. K. Chembo, "On the phase noise performance of microwave and millimeter-wave signals generated with versatile Kerr optical frequency combs," *Opt. Exp.*, vol. 24, no. 22, p. 25043, 2016.
[28] J. Liu, E. Lucas, A. S. Raja, J. He, J. Riemensberger, R. N. Wang, M. Karpov, H. Guo, R. Bouchand, and T. J. Kippenberg, "Photonic microwave generation in the X- and K-band using integrated soliton microcombs," *Nature Photon.*, vol. 14, no. 8, pp. 486–491, Aug. 2020.
[29] K. Zeb, Z. Lu, J. Liu, Y. Mao, G. Liu, P. J. Poole, M. Rahim, G. Pakulski, P. Barrios, M. Vachon, D. Poitras, W. Jiang, J. Weber, X. Zhang, and J. Yao, "Broadband optical heterodyne millimeter-wave-over-fiber wireless links based on a quantum dash dual-wavelength DFB laser," *J. Lightw. Technol.*, vol. 40, no. 12, pp. 3698–3708, Jun. 15, 2022.
[30] E. Saia Lima, N. Andriolli, E. Conforti, G. Contestabile, and A. Cerqueira Sodré, "Low-phase-noise tenfold frequency multiplication based on integrated optical frequency combs," *IEEE Photon. Technol. Lett.*, vol. 34, no. 16, pp. 878–881, Aug. 15, 2022.
[31] E. S. Lima, R. M. Borges, N. Andriolli, E. Conforti, G. Contestabile, and A. C. Sodré, "Integrated optical frequency comb for 5G NR Xhauls," *Sci. Rep.*, vol. 12, no. 1, p. 16421, Sep. 2022.
[32] M. Smit et al., "An introduction to InP-based generic integration technology," *Semicond. Sci. Technol.*, vol. 29, no. 8, p. 083001, Jun. 2014.
[33] R. H. D. Souza, O. L. Coutinho, J. E. B. Oliveira, A. A. Ferreira, and J. A. J. Ribeiro, "An analytical solution for fiber optic links with photonic-assisted millimeter wave upconversion due to MZM nonlinearities," *J. Microw., Optoelectron. Electromagn. Appl.*, vol. 16, no. 1, pp. 237–258, Mar. 2017.
[34] J. Oh and T.-K. Kim, "Phase noise effect on millimeter-wave pre-5G systems," *IEEE Access*, vol. 8, pp. 187902–187913, 2020.

EDUARDO SAIA LIMA received the B.Sc., M.Sc., and Ph.D. degrees in telecommunications engineering from the National Institute of Telecommunications (Inatel), Brazil, in 2017, 2019, and 2023, respectively. He is currently an Innovation and 5G Coordinator with VS Telecom. Since 2017, he has been a Professor in the Teaching Internship Program and as a Researcher with the Laboratory Wireless and Optical Convergent Access (WOCA), Inatel. He has coauthored more than 40 papers published in international peer-reviewed journals and presented at leading international conferences. His research interests include microwave photonics and optics communications applied to 5G systems, radio-over-fiber (RoF), fiber-wireless systems, free-space optics (FSO), power-over-fiber (PoF), visible light communication (VLC), photonic integrated circuits, and Li-Fi (light-fidelity).

TOMÁS POWELL VILLENA ANDRADE received the B.Sc. degree in engineering physics from the National University of Engineering (UNI), Lima–Peru, and the M.Sc. degree from Unicamp, Brazil, in 2011. He is currently pursuing the Ph.D. degree in telecommunications engineering with the National Institute of Telecommunications (Inatel), Brazil. He is also a Researcher of the Brazil 6G Project with the Laboratory WOCA, Inatel. His research interests include embedded electronics, microwave photonics, and integrated photonics for telecommunications applications.

NICOLA ANDRIOLLI received the Laurea degree in telecommunications engineering from the University of Pisa, in 2002, and the Diploma and Ph.D. degrees from Scuola Superiore Sant'Anna, Pisa, in 2003 and 2006, respectively. He was a Visiting Student with DTU, Copenhagen, Denmark, and a Guest Researcher with NICT, Tokyo, Japan. From 2007 to 2019, he was an Assistant Professor with Scuola Superiore Sant'Anna. Since 2019, he has been a Researcher with CNR-IEIIT. He authored more than 200 publications in international journals and conferences, contributed to one IETF RFC, and filed 11 patents. He has a background in the design and the performance analysis of optical circuit-switched and packet-switched networks and nodes. His research interests include photonic integration technologies for telecom, datacom, and computing applications, working in the field of optical communications, processing, and computing.

EVANDRO CONFORTI (Life Senior Member, IEEE) received the B.Sc. degree in electronic engineering from the Technological Institute of Aeronautics (ITA), Brazil, in 1970, the M.Eng. degree from the Federal University of Paraiba, Brazil, in 1972, the M.A.Sc. degree from the University of Toronto, Canada, in 1978, and the Ph.D. degree in electrical engineering from the University of Campinas (Unicamp), Campinas, Brazil, in 1983. He was a Visitor with the University of Illinois at Urbana–Champaign, IL, USA, from 1992 to 1994, working with the Research Team of Prof. S. M. (Steve) Kang. He has graduated 15 Ph.D. students and 32 M.Sc. students. He has been with Unicamp, since 1981, where he was the Dean of the Faculty of Electrical and Computer Engineering (FEEC), from 1984 to 1987. He is currently an Invited Professor of electrical engineering with FEEC. He holds 17 patents (11 awarded) and is the coauthor of a book and more than 200 papers in Brazilian and International Journals and Conferences. His research interests include semiconductor optical amplifiers (SOAs), photonic integrated circuits (PICs), optical coherent communication, electro-optical switching, and electromagnetic measurements. He received the ''Unicamp Inventors Prize,'' in 2013, 2016, 2018, and 2020; the ''Academic Merit Medal Prof. A. J. Giarola,'' Brazilian Society of Microwaves and Optoelectronic, in 2014; the ''First Werner von Siemens Technologic Innovation Prize'' (3° place Cat. Researcher) from Siemens, Brazil, in 2005; the ''Zeferino Vaz Academic Achievements Prize'' from Unicamp, in 2005; the ''1998 Brazilian Invention Prize''; and the ''1983 Unicamp Research Prize.'' His Ph.D. supervised students received the ''first place IMOC 2017 Student Paper Competition,'' the ''Best Electrical Engineering Thesis'' from CAPES, Brazil, in 2010, and the ''2002 IEEE/LEOS Graduate Student Fellowship.''

GIAMPIERO CONTESTABILE received the Laurea degree in physics from the Sapienza University of Rome, Rome, Italy, in 1998, and the Ph.D. degree in electrical engineering and telecommunications from the University of Rome ''Tor Vergata,'' in 2001. From 1996 to 2000, he was with the Semiconductor Devices Group, Fondazione Ugo Bordoni, Rome. In 2001, he was with Opto Speed Italia. He is currently an Associate Professor with Scuola Superiore Sant'Anna, Pisa, Italy. He has coauthored more than 200 papers published in international peer-reviewed journals and presented in leading international conferences. His research interests include photonic integrated circuits, advanced optical systems, access networks, and semiconductor optical amplifiers and lasers.

ARISMAR CERQUEIRA S. JR. received the B.Sc. degree in electrical engineering from the Federal University of Bahia, Brazil, in 2001, the M.Sc. degree from Unicamp, Brazil, in 2002, and the Ph.D. degree from Scuola Superiore Sant'Anna, Italy, in 2006. He was a Invited Researcher and a Professor from many world-recognized universities, such as the University of Oulu, in 2017, Scuola Superiore Sant'Anna, in 2015, 2017, and 2019; Danish Technical University, Denmark, in 2013; Max-Planck Institute, Germany, in 2010; and the University of Bath, U.K., in 2004, 2005, and 2007. He was an Associate Professor with Unicamp, from March 2009 to August 2011. He joined the Brazilian National Institute of Telecommunications (Inatel), as an Associate Professor. Since 2009, he has been a Coordinator of the Research and Development Projects on diverse areas of telecommunications, including 5G, 6G, antennas, radars, and microwave photonics. He is a holder of 11 patents, has transferred 25 products to the industry and has published more than 300 scientific articles.

Open Access funding provided by 'Consiglio Nazionale delle Ricerche-CARI-CARE-ITALY' within the CRUI CARE Agreement